Open Research Online

The Open University's repository of research publications
and other research outputs

Near IR spectroscopy of candidate B[e]/X-ray binaries

Journal Item

For guidance on citations see FAQs.

Version: Version of Record

Link(s) to article on publisher's website:
http://aa.springer.de/papers/9348003/2300888.pdf

oro.open.ac.uk

Near IR spectroscopy of candidate B[e]/X-ray binaries

J.S. Clark[1], **I.A. Steele**[2], **R.P. Fender**[3], and **M.J. Coe**[4]

[1] Astronomy Centre, CPES, University of Sussex, Brighton, BN1 9QH, UK
[2] Astrophysics Research Institute, Liverpool John Moores University, Liverpool, L41 1LD, UK
[3] Astronomical Institute Anton Pannekoek, University of Amsterdam and Center for High Energy Astrophysics, Kruislaan 403, 1098 SJ Amsterdam, The Netherlands
[4] Department of Physics and Astronomy, Southampton University, Highfield, Southampton, UK

Abstract. We present near IR spectra (0.8–2.5 μm) of the two candidate B[e]/X-ray binary systems CI Cam/XTE J0421+560 and HD34921/1H 0521+37. The spectra of both systems show evidence for a more complex circumstellar environment than those seen in classical Be/X-ray binaries. Strong H I and He I emission is seen, confirming the presence of a dense circumstellar wind; O I, Fe II and [Fe II] emission in CI Cam points to recombination of this wind. He II emission, presumably due to excitation by the compact companion is observed in CI Cam. Finally, emission is seen from Na I and CO, which implies regions of the circumstellar environment with much lower excitation temperatures and higher densities, shielded from direct stellar radiation. Both systems show evidence for continuum emission from circumstellar dust. Neither of these two features has previously been observed in any other classical Be/X-ray binary system. Adopting the classification criteria of Lamers et al. (1998) we suggest identifications of unclB[e] and sgB[e] for HD34921 and CI Cam respectively, making them the first High Mass X-ray Binaries with primaries showing the B[e] phenomenon known.

Key words: stars: circumstellar matter – stars: emission-line, Be

1. Introduction

To date no High Mass X-ray Binary (HMXB) has been observed with a B[e] star as the mass donor. B[e] stars differ from classical Be stars in that they show a pronounced near IR excess due to emission from warm dust rather than from the free–free and bound–free emission from the gaseous envelope of classical Be stars. Both classical Be stars and B[e] stars have rich emission spectra, although B[e] stars also show forbidden emission lines in their spectra. As a class of object, B[e] stars are rather heterogeneous, with many objects of differing evolutionary states classified as such (eg Lamers et al. 1998; henceforth L98). One such evolutionary state is the supergiant B[e] star (henceforth

sgB[e] star; notation from L98). First identified in the Magellanic Clouds by Zickgraff et al. (1985) these stars are thought to represent an intermediate post Main Sequence evolutionary stage between OB supergiants and the Hydrogen depleted Wolf Rayet stars. Since HMXB systems with both supergiant and Wolf Rayet primaries have been identified it seems natural to suppose that HMXB's with sgB[e] primaries also exist.

One possible B[e]/ X-ray binary candidate is CI Cam (=MWC 84), which was recently proposed as the optical counterpart to the transient X-ray source XTE J0421+560 by Wagner et al. (1998). XTE J0421+560 was first detected by the RXTE All-Sky Monitor on 1998 March 31 with a peak flux on 1998 April 1 of $\sim$2 Crab in the 2–12 keV band (Smith et al. 1998). Emission at energies of up to 70 keV was also detected by the Burst and Transient Source Experiment (BATSE) experiment aboard the Compton Gamma Ray Observatory (CGRO). Optical spectroscopy at this time revealed a rich emission line spectrum, similar to that reported by Downes (1984), but with the presence of additional He II emission features. Hjellming & Mioduszewski (1998) reported the detection of a transient 19 mJy source at 1.4 GHz, corresponding to the optical position of CI Cam on 1998 April 1, which subsequently brightened considerably. Optical/near IR photometry of the source (Clark et al., in prep.) showed that the star had brightened by $\sim$2–3 magnitudes at this time, confirming this as the optical counterpart to XTE J0421+560.

Another candidate B[e] star is HD 34921, the proposed optical counterpart to 1H 0521+37 (Polcaro et al. 1990). Although tentatively identified as a B0 II-IVpe star, HD 34921 has been identified positionally with the IRAS point source 051921+3737 (Polcaro et al. 1990); to the best of our knowledge no classical Be/X-ray binary shows evidence for emission from circumstellar dust. Optical spectra of the source show variable He II emission (Polcaro et al. 1990), possibly originating in either a circumstellar envelope/compact object interaction, or an accretion disc. We note that variable He II emission features are not seen in any other classical Be/X-ray binary system (although we note that there is some evidence for infilling of the He II 4686Å line in X Per; Lyubmikov et al. 1997).

We present near IR spectra (0.8–2.5 μm) spectra of the 2 candidate B[e]/X-ray binaries to determine the composition of, and conditions present in their circumstellar envelopes, and hence to classify the mass donors in both systems. Near IR spectroscopy is a powerful technique to accomplish this due to the presence of emission features from both high (eg He II, N II and C IV) and low (Na I and CO bandhead) excitation species within the J, H and K bands.

2. Observations and reduction strategies

The J, H and K band spectra presented here (Figs. 1–6) were obtained with the Cooled Grating Spectrometer 4 (CGS4; Mountain et al. 1990) of the United Kingdom Infrared Telescope (UKIRT), Mauna Kea, Hawaii, in both observer led and service modes. CGS4 provides spectral coverage from 1 to 5 μm and the observations described here were made using the 256×256 pixel infrared array as a detector. Initial data reduction was carried out at the telescope using the CGS4DR software (Puxley et al. 1992). This removes bad pixels, debiases, flat-fields, linearity corrects and interleaves oversampled scan positions. The subsequent stages of data reduction were carried out using the Starlink-supported package FIGARO. In order to ensure accurate removal of atmospheric features from the spectra we followed a procedure similar to that outlined by Hanson et al. (1996; henceforth H96). An A0 - A3 III-V standard star was observed after each target at an airmass within 0.1 of the target. Once per hour observations were also taken of a G2–3V star.

The K band spectra of HD 34921 were obtained in service time on 1992 January 13 and 1993 November 11, and the J, H and K band spectra of CI Cam were also obtained in service time on the nights of 1998 April 4 (J and K band) and 5 (H band). By comparison the peak X-ray flux of the flare occurred on April 1, and the broadband UBVR and 15 and 8 GHz fluxes were all declining by this time Clark et al., in preparation).

Finally the I band spectrum of HD 34921 was obtained on 1993 December 12 using the 1-m Jacobus Kapteyn Telescope (JKT) at La Palma with the Richardson-Brearly spectrograph and the 1200 lines/mm grating, with FIGARO being used in the data reduction.

We present the spectra in Figs. 1–6, and summarise the line identifications for each object in Tables 1–6. Identifications were based on the lines listed in Kelly et al. (1994; henceforth KRC94), Hamann et al. (1994) and Morris et al. (1996). The spectra were analysed with the routine SPLOT in IRAF, which was used to deconvolve blended profiles where possible by fitting gaussian line profiles from which line fluxes and equivalent widths (EW) were measured.

Special mention must be given to the analysis of the CI Cam spectra. Although listed, EW from different wavebands are not directly comparable due to the rapidly varying continuum level during the outburst. Equally, the rich emission line spectrum presented considerable problems given the relatively low resolution of the observations, and the inevitable blending of emission features. Where possible these blends were deconvolved as described above. However, in certain cases such as the He I
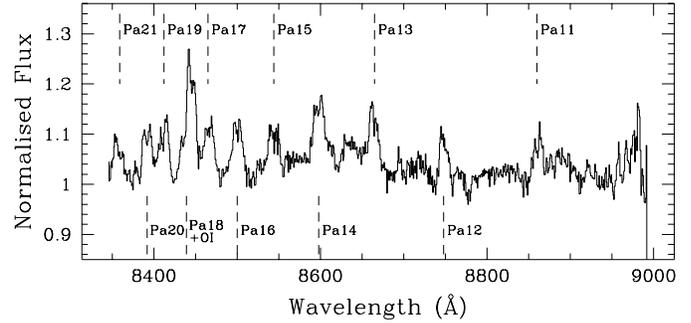

Fig. 1. I band spectrum of HD34921/1H0521+373. Wavelength in Å given on the horizontal axis, normalised flux given on the vertical axis. The rest wavelengths of the Paschen series transitions and O I 8446Å feature indicated by the broken lines.

Table 1. 8300–9000Å line identifications for HD34921/1H0521+37 (wavelengths are given in microns; EW in -Å).

Wavelength	Feature	EW
~8359	Pa21	0.8
~8392	Pa20	1.3
~8412	Pa19	1.5
~8439	Pa18+O I (8446)	3.3
~8465	Pa17	1.6
~8500	Pa16(+Ca II?)	1.7
~8544	Pa15(+Ca II?)	1.6
~8598	Pa14(+[Fe II]?)	2.2
~8665	Pa13 (+Ca II?)	2.0
~8748	Pa12	1.4
~8860	Pa11	1.3

1.083 and 2.058 μm complexes this was not possible. In these cases we have listed the total EW and flux under the strongest transition of that complex. We find a total of 122 possible transitions, and identify 88 of these. We tentatively identify a further 11 lines (those marked with a '?' in Tables 5–7), leaving a total of 23 unidentified. In addition there are a number of other possible features in the spectra at a low level for which identification has not been attempted (e.g. in the region ~1.2–1.24 μm). All EW and fluxes are given to two significant figures in Tables 5–7; we estimate errors of the order of ~10 per cent for both EW and line fluxes.

CO bandhead EW and fluxes were measured between 2.285–2.314 μm (2-0), 2.314–2.342 μm (3-1) and 2.342–2.370 μm (4-2). Although additional emission features were clearly present redwards of ~2.35 μm no attempt was made to derive EW or fluxes for these given the low resolution and S/N ratio of the spectrum in this region.

3. HD34921/1H0521+37

The I band spectrum (Fig. 1) shows the Paschen series from Pa21-Pa11 to be in emission. The lines are clearly resolved, and show the double peaked profile characteristic of emission from a circumstellar disc. An average peak separation of ~300±10 kms^{-1} is measured; adopting canonical values for
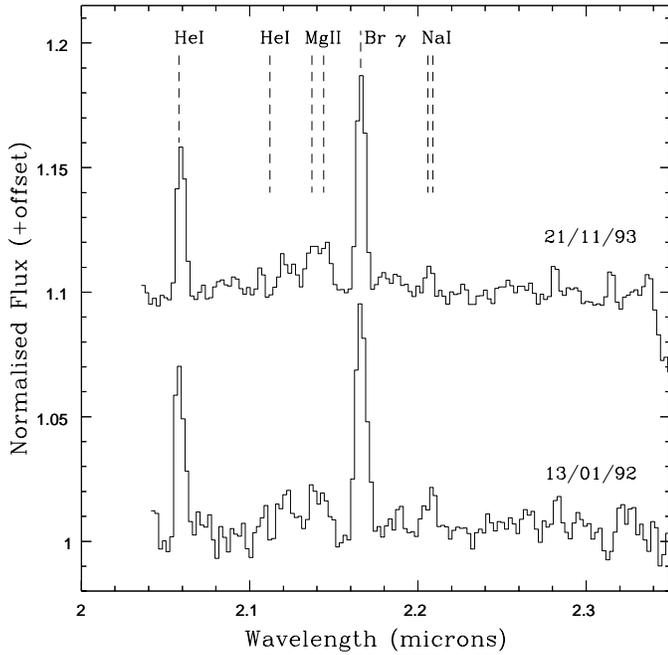
Fig. 2. K band spectra of HD34921/1H0521+373. Wavelength in Å given on the horizontal axis, normalised flux given on the vertical axis. The positions of the various hydrogen, helium and metallic transitions indicated by broken lines.
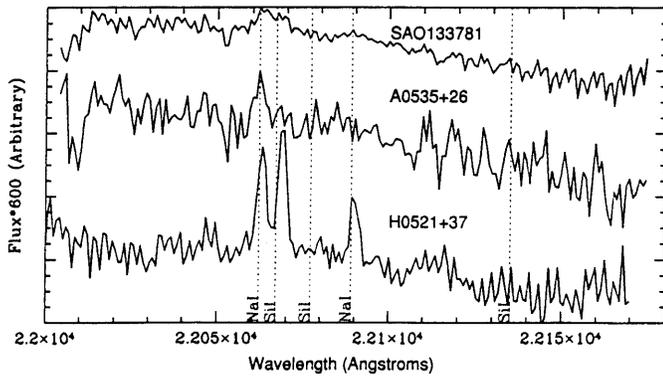

Fig. 3. Echelle spectrum of HD34921/1H0521+373, confirming the presence of Na I emission (reproduced, with kind permission from Everall 1995).

Table 2. K band line identifications for HD34921/1H0521+37. Wavelengths are given in microns; EW in -Å, **bl** indicating a blend.

Wavelength	Feature	EW:(13/1/92)	(21/11/93)
2.059	He I 2.058	4.4	3.9
2.136	Mg II 2.137	2.8	2.5
2.144	Mg II 2.144	bl	bl
2.166	Brγ	7.1	5.4
2.204	Na I 2.206	bl	bl
2.209	Na I 2.209	1.3	0.5

Table 3. J band line identifications for CI Cam (1998 April 4). Wavelengths are given in microns; EW in -Å and fluxes in milliJansky. Line identifications with a question mark indicate uncertainty; transitions with no identification are simply marked with a question mark.

Wavelength	Feature	EW	Flux
1.0307	He I (74) ($3p^3P^0$-$6d^3D$) 1.311?	2.0	2.6
1.0400	Fe II ($5s^6D_{9/2}$-$4p^6F^0_{9/2}$) 1.0402	0.6	0.7
1.0457	[Ni II] ($a^2F_{7/2}$-$b^2D_{5/2}$) 1.0459?	0.7	0.9
1.0501	Fe II (z^4F_7-b^4G_9) 1.0501	4.0	4.7
1.0688	C I 1.0683, 85, 91?	bl	bl
1.0728	N I 1.074?	bl	bl
1.0829	He I ($2s^3S$-$2p^3P^0$) 1.083	337.8	524.0
1.0917	He I (3^1D-6^1F^0) 1.0917	bl	bl
1.0939	Pa (6-3) 1.0938	bl	bl
1.1024	?	bl	bl
1.1042	He I ($3p^1P^0$-$6d^1D$) 1.1045	bl	bl
1.1127	Fe II (z^4F_3 - b^4G_5) 1.1126	1.0	2.4
1.1290	O I ($3p^3P$ - $3d^3D^0$) 1.129	10.0	16.9
1.1332	?	2	2.8
1.1385	Na I ($4s^2S$ - $3p^2P_0$) 1.1384	0.4	0.8
1.1407	Na I ($4s^2S$ - $3p^2P_0$) 1.1407	0.6	1.1
1.1627	He II (7-5) 1.1628	1.0	2.0
1.1665	Fe II 1.166	1.0	2.0
1.1755	C I (24) 1.1754, 53, 48	4.0	6.9
1.1841	?	0.7	1.4
1.1894	[Fe II] (a^4D_7 - a^2G_7) 1.1881?	0.7	1.5
1.1970	He I ($3p^3P^0$ - $5d^3D$) 1.1970	3.0	6.2
1.2034	?	0.2	0.4
1.2086	?	0.3	0.6
1.2467	N I (36) ($3p^2D_{3/2}$-$3d^2F_{7/2}$) 1.2469	0.8	1.8
1.2526	He I ($3s^3S$ - $4p^3P^0$) 1.2528	4.0	8.5
1.2566	[Fe II] (a^6D_9 - a^4D_7) 1.2567	0.7	1.8
1.2611	?	0.4	1.0
1.2786	He I ($3d^3D$ - $5f^3F^0$) 1.2748	5.0	14.0
1.2819	Pa (5-3) 1.2822	13	34.5
1.2967	He I ($3p^1P^0$ - $5d^1D$) 1.2968	2.0	5.4
1.3166	O I (3^3P - 4^3S) 1.3165	0.6	1.6

the mass and radius of a B0IV star we determine that this velocity corresponds to the Keplerian velocity of material orbiting at ≤ 5.5 R$_*$. The only other prominent line in the spectrum is O I 8446 Å, which is blended with Pa18. This is seen in 23 out of 40 Be stars (Andrillat et al. 1988), and is likely populated by Lyβ fluorescence. Fe II at 8515 and 8599 Å is not present above the level of noise (the optical spectra show no evidence for Fe II emission; Polcaro et al. 1990). If present [Fe II] 8599 Å is blended with Pa14, as are the 3 Ca II transitions within this spectral region.

Since the S/N ratios of the 2 K band spectra are not high we present both so that a comparison between the spectra can be made (Fig. 2). He I 2.058 μm and Brγ are clearly in emission.

However, there is no evidence of absorption or emission in the He I 2.112 μm line. Comparison of the two spectra suggests emission in the Mg II 2.138/2.144 μm and Na I 2.206/2.209 μm lines. The 2 Mg II transitions are thought to be populated by Lyβ fluorescence (e.g. McGregor et al. 1988; henceforth MHH88), and are seen in emission in a number of both main sequence Be and post main sequence objects (Clark et al., in prep.; MHH88).

Table 4. H band line identifications for CI Cam (1998 April 5). Wavelengths are given in microns; EW in -Å and fluxes in milliJansky. Line identifications with a question mark indicate uncertainty; transitions with no identification are simply marked with a question mark.

Wavelength	Feature	EW	Flux
1.4297	?	0.5	1.2
1.4414	?	2.0	5.0
1.4542	?	2.0	5.0
1.4764	He II (9-6) 1.4765?	0.3	0.9
1.4879	He II (14-7) 1.4882	0.3	0.9
1.5087	He I ($4p^1P^0$ -$3s^1S$)	1.0	2.5
	+ Br (22-4)		
1.5134	Br (21-4) 1.5314	0.1	0.4
1.5194	Br (20-4) 1.5192	0.1	0.3
1.5264	Br (19-4) 1.5265	0.1	0.4
1.5345	Br (18-4) 1.5346	0.2	0.5
1.5444	Br (17-4) 1.5443	0.3	0.9
1.5567	Br (16-4) 1.5561	0.6	2.3
1.5704	Br (15-4) 1.5705	0.6	2.2
1.5773	Fe II ($z^2I_{11/2}$ - $3d^54s^2I_{11/2}$) 1.5776	0.6	2.2
1.5884	Br (14-4) 1.5885	0.9	3.5
1.5965	[Fe II] ($a^4F_{7/2}$-$a^4D_{3/2}$) 1.598?	0.1	0.3
1.6019	[Fe II] ($a^4F_{7/2}$ - $a^4D_{3/2}$)1.601	0.2	0.7
1.6116	Br (13-4) 1.6114	0.6	2.6
1.6412	Br (12-4) 1.6412	0.8	3.7
1.6807	Br (11-4) 1.6811	1.2	6.2
1.6894	Fe II ($z^4F_{9/2}$-$c^4F_{9/2}$) 1.688	1.2	6.8
	+He II (12-7) 1.692		
1.7006	He I ($4p^3P^0$ - $3s^3S$) 1.7007	4.0	19.3
1.7358	Br (10-4) 1.7362	2.0	11.2
1.7451	[Fe II] (a^4F_3 - a^4D_1) 1.7449	0.5	2.7
1.7780	?	0.1	0.7
1.7830	?	0.5	3.0
1.8029	?	bl	bl
1.8173	Br (9-4) 1.8179	3.2	19.8
1.8228	?	bl	bl
~1.8565	He I 1.8561?	bl	bl
1.8639	He II (6-5) 1.8639	3.0	22.9
1.8695	blend of He I 1.8681/1.8702?	6.0	40.6
1.8750	Pa (4-3) 1.8751	14	96.5
1.8816	?	0.8	5.0
1.8942	?	0.2	1.4
1.9087	He I 1.9068/94	2.0	17.6
1.9435	Br (8-4) 1.9451	2.0	16.8
1.9541	He I ($4p^3P$ - $3d^3D$) 1.9548?	1.0	9.9
1.9738	Fe II (z^4F_5 - c^4F_5) 1.9746?	0.2	1.9

Table 5. K band line identifications for CI Cam (1998 April 4). Wavelengths are given in microns; EW in -Å and fluxes in milliJansky. features longwards of ~2.35 μm not listed separately; see Sect. 4. Line identifications with a question mark indicate uncertainty; transitions with no identification are simply marked with a question mark.

Wavelength	Feature	EW	Flux
1.9855	?	0.3	3.0
1.9958	?	0.1	0.8
2.0071	?	0.1	0.9
~2.02-2.05	blend	bl	bl
2.059	He I ($2s^1S$ - $2p^1P^0$) 2.058	26	287.7
2.6613	He I ($4s^1S$ - $3d^1D$) 2.068	bl	bl
2.0907	Fe II ($z^4F^0_{3/2}$ - $c^4F_{3/2}$) 2.091	0.1	1.2
2.1127	He I ($3p^3P^0$ - $4s^3S$) 2.112	2.0	17.8
	+ He I ($3p^1P^0$ - $4s^1S$) 2.113		
2.1274	?	0.1	0.8
2.1376	Mg II ($5s^2S_{1/2}$ - $5p^2P^0_{1/2}$) 2.138	0.15	1.4
2.1447	Mg II ($5s^2S_{1/2}$ - $5p^2P^0_{1/2}$) 2.144	0.3	3.8
2.1487	He I ($4p^3P$ - $7s^3S$) 2.15?	0.3	3.8
2.1570	?	0.2	2.1
2.1610	He I ($4d^1D$ - $7f^1F$) 2.1614	0.6	7.3
2.1663	Brγ 2.1661	2.0	26.5
2.1834	?	0.2	2.0
2.1883	He II (10-7) 2.189	0.1	0.8
2.207	Na I ($4p^2P^0_{3/2}$ - $4s^2S_{1/2}$ 2.206)	0.4	5.6
	+Na I ($4p^2P^0_{3/2}$ - $4s^2S_{1/2}$ 2.209)		
2.2543	[Fe II] ($a^2G_{7/2}$ - $a^2H_{5/2}$) 2.2540	0.1	1.3
2.2643	[Fe II] ($b^2H_{7/2}$ - $b^2G_{7/2}$) 2.2661?	0.1	1.1
2.2721	?	0.1	0.8
2.2811	?	0.1	1.1
~2.295	CO (2-0) bandhead	0.3	4.6
~2.323	CO (3-1) bandhead	0.3	4.3
~2.354	CO (4-2) bandhead	0.3	4.8

same night and reduced in the same fashion are also shown to demonstrate that this is unlikely to be an artifact). The 2 Na I features are very narrow, with a FWHM<50 kms^{-1}; assuming kinematical broadening this implying a very low projected velocity for the emitting region.

Features at ~2.12 and ~2.28 μm seem to be present in both observations. To the best of our knowledge no feature at ~2.28 μm is seen in any other Be or early type star. The feature at 2.12 μm may be H_2 emission, which is often an indication of shocked material. However no [Fe II] features, which are also associated with shocked emission are seen; we therefore refrain from further discussion until higher resolution and S/N ratio spectra are available.

3.1. Dust emission?

Polcaro et al. (1990) suggests that HD34921 is associated with the IRAS source 051921+3737 which has the characteristic colours of emission from cold dust. Adopting the distance to 1H0521+37 of 1.7±0.1 kpc given in Polcaro et al. (1990), we can derive an order of magnitude estimate for the mass of the (possibly) circumstellar dust. From the method of Soifer et al.
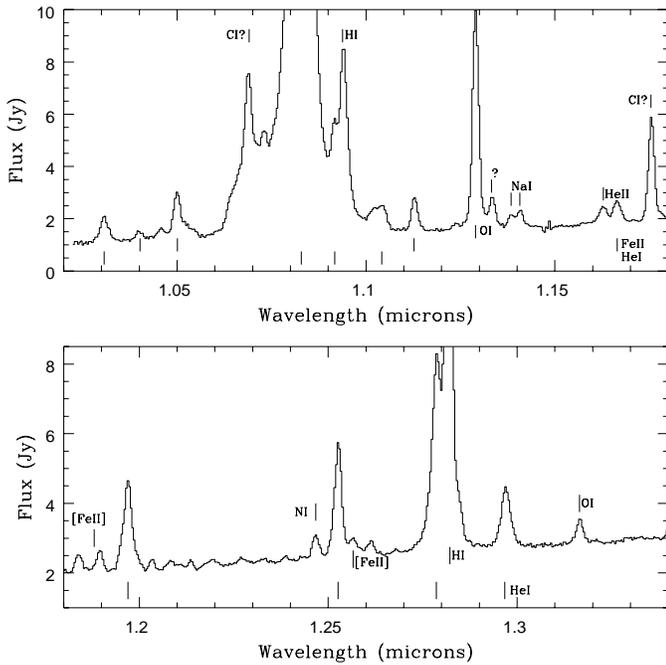
The presence of Na I emission is confirmed by an echelle spectrum of the region obtained on 1993 January 18 and presented in Everall (1995; reproduced in Fig. 3), which clearly shows two narrow emission peaks at the rest wavelengths of the Na I transitions. A third feature at ~2.2069 μm is unlikely to be doppler shifted emission from the 2.206 μm line given that a corresponding component is not seen redwards of the 2.209 μm line. An identification with Si I 2.2067 μm is possible, but also appears unlikely given that the other two transitions from this series are absent (the spectra of two other stars taken on the

Fig. 4. J band spectrum of CI Cam; note the differing ranges of the flux (in Jy) on the vertical axes of the 2 plots. The wavelength is given in microns in both panels. The central wavelength of the features present in the spectra are indicated by tickmarks; where the feature is identifiable it is labeled (a question mark indicating an unidentifiable feature).

Fig. 5. H band spectrum of CI Cam; wavelength and flux units as given in Fig. 4. Emission features are identified following the notation of Fig. 4.

(1986), using the 100 μm flux reported by Polcaro et al. (1990), a mass absorption coefficient derived from Soifer et al. (1986), and an estimated dust temperature of $\sim$50 K we find a dust mass of $\sim 10^{-4}$ M$_\odot$. The largest source of error lies in the difficulty in deriving a temperature for the dust given that the short wavelength data is likely dominated by free free and bound free emission and longer wavelength data is sparse. Additional sources of error include the distance estimate, and the extrapolated value for the mass absorption coefficient (where the mass absorption coefficient is assumed to vary as $\lambda^{-1.5}$ at wavelengths $>$20 μm; Soifer et al. 1986). Assuming a gas to dust ratio of 100:1 we derive an estimate of 10^{-2} M$_\odot$ for the total mass of ejecta associated with the cold dust. Adopting a mass loss rate for the Be star of 10^{-7}-10^{-8} M$_\odot$ yr^{-1} (e.g. Waters 1986) such a mass would take 10^5-10^6years to accumulate. Given the lifetime for a B0 star is of the order of 10^7 years such a mass could be lost via the stellar wind of the star (Maeder & Maynet 1989).

4. CI Cam

The J, H & K band spectra of CI Cam are presented in Figs. 4–6. The rich near IR emission spectra of CI Cam confirm the presence of several physically distinct regions in the circumstellar envelope; below we summarise the main features of the spectra; a comprehensive line list is provided in Tables 5–7.
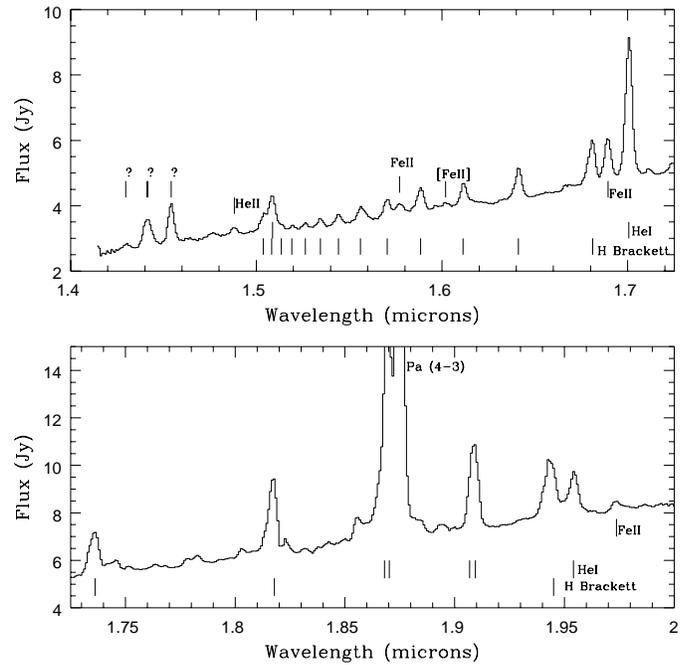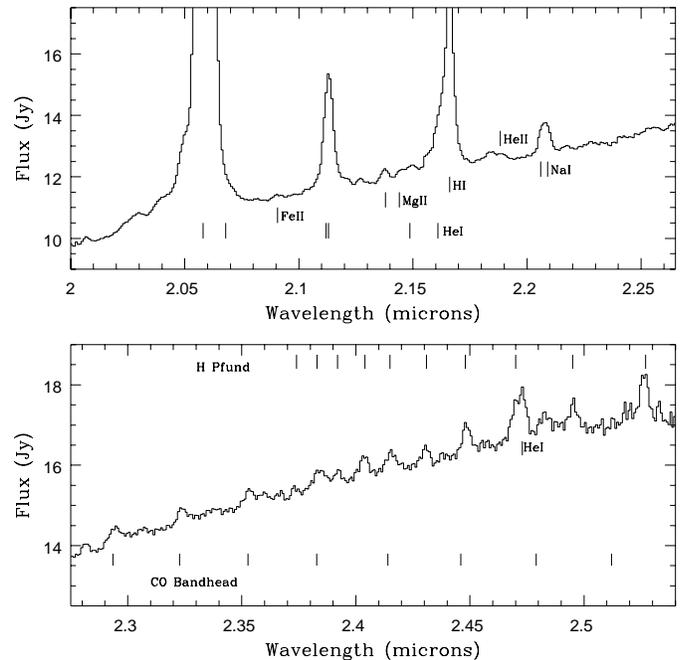

Fig. 6. K band spectrum of CI Cam; wavelength and flux units as given in Fig. 4. Emission features are identified following the notation of Fig. 4.

4.1. Hydrogen and helium emission

Strong H I emission is seen throughout the near IR spectrum of CI Cam. The lower Paschen series of hydrogen is in emission, as is the Bracket series up to Br21, and the Pfund series to Pf25. Assuming $E(B - V) = 0.65 \pm 0.2$ Clark et al., in
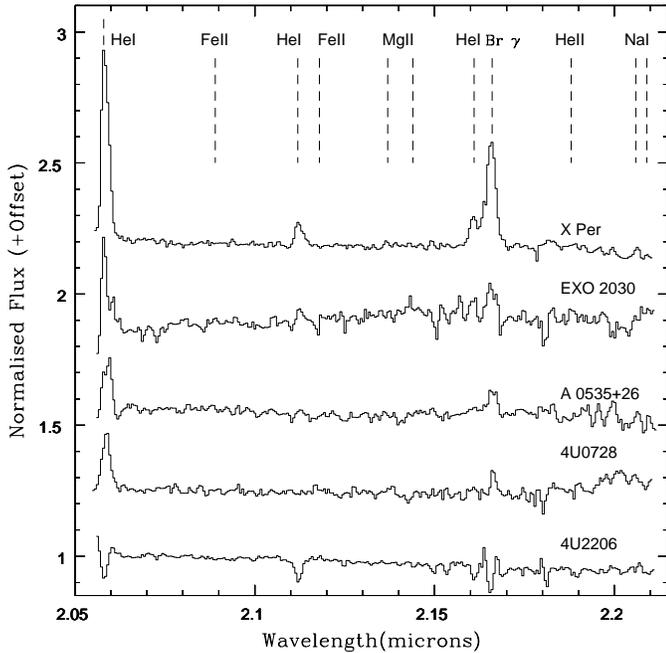
Fig. 7. K band spectra of the Be/X-ray binary systems taken between 1996 October 1–3. Line identifications indicated by tickmarks, EW given in Table 1.

preparation) the line ratios of the Brackett series in the H band observations are consistent with case B nebular recombination for $N_e > 10^4$ cm^{-3} and T$> 10^4$ K. He I emission is also seen throughout the spectrum; the 1.0830 and 2.058 μm transitions are the strongest lines observed in the near IR spectrum of CI Cam. The upper state of He I 1.083 μm line can be populated by recombination, and also via collision from the $2s^3$S state, so contributions to the line flux can be provided from both singly ionised and neutral regions. The 2.058 μm transition is the singlet equivalent of the 1.083 μm line, and is primarily populated via recombination. However, a large optical depth at 584 Å is required to drive the line into emission since the 2^1P-1^1S resonance line transition at this wavelength is 10^3 times more likely than the 2^1P-2^1S 2.058 μm transition. In practice this implies a limited effective temperature range for the transition; too cool and there is insufficient ionisation; too hot and the majority of the helium is ionised reducing the optical depth at 584 Å and thus favouring the 2^1P-1^1S transition. Given the population mechanisms of these transition, and the highly variable ionisation conditions at the time of the X-ray outburst, they do not serve as useful indicators of circumstellar conditions. Strong He I emission at 1.197, 1.700 and 2.112 μm is also observed; most likely predominantly populated via recombination. After dereddening, flux ratios of He I 1.197 μm/Pa$\beta \sim$0.18 and He I 1.700 μm /Br$\gamma \sim$0.73 are obtained, comparable to those measured for the LBV AG Car (MHH88). He II emission features are seen at 1.626 μm (7-5), 1.5719 μm (13-7) and 2.1885 μm (10-7), with transitions at 1.2813 μm and 1.6918 μm probably blended with other emission features.

4.2. Na I and CO bandhead emission

Na I is observed in emission at 1.1385, 1.1407 and 2.206/9 μm; the emission must arise in regions shielded from both direct stellar radiation and radiation from the vicinity of the compact object, which would quickly ionise Sodium (following the arguments of Hamann & Simon 1986 for MWC 349, the Na I emission region must be cooler and/or denser than the Fe II region). A similar conclusion can be drawn from the presence of CO bandhead emission.

Given that the flux measured for the (2-0) and (4-2) bandheads is $\sim$equal we conclude from the analysis of Scoville et al. (1980) that the CO bandhead emission is due to collisional excitation rather than UV excitation. This implies temperatures of $\sim$3000-5000 K, and densities $\geq 10^{10}$ cm^{-3} for the emitting region. As is the case for Na I emission, the implied density far exceeds that derived for the regions giving rise to the Fe II and [Fe II] emission.

Following the analysis of Oudmaijer et al. (1995) we can derive minimum radii for the CO bandhead emitting regions assuming that the emission is optically thick. The black body radius is given by

$$F_L = N_{line} B_\nu(\nu, T) \Delta\nu\pi \left(\frac{R_{BB}}{d}\right)^2 \qquad (1)$$

where F_L is the bandhead flux in Wm^{-2}, $\Delta\nu$ the line width of the individual line (assumed to be 10 kms^{-1}), N_{line} the number of lines contributing to the flux (assumed to be 50), B$_\nu$ the Planck function, d the distance to CI Cam and R_{BB} the radius of the emitting region. We further adopt the assumption of Oudmaijer et al. (1995) of an average line separation of 35 kms^{-1}; therefore if we have underestimated the width of the individual lines we will have overestimated the size of the emitting region by at most a factor of $\sim$2. Assuming that CI Cam lies at a distance of 2 kpc (Clark et al., in preparation) we derive a radius for the emitting region of $\sim$120 R$_\odot$.

4.3. Other emission lines

Fe II and [Fe II] emission is seen throughout the spectrum. The Fe II lines are likely populated by Lyα fluorescence (Hamann et al. 1994), suggesting their origin in a dense partially ionised region, such that there is a large population of Fe II and Lyα photons. This region is probably the same one that gives rise to the O I emission (see below); the presence of Fe II in emission then implies densities $> 10^{5-6}$ cm^{-3} for this zone (Hamann et al. 1994). The 1.2941/1.2567 μm [Fe II] line ratio implies a density for the forbidden line emission region of $\leq 10^5$ cm^{-3}. Optical spectroscopy shows that the line profiles for the permitted and forbidden regions differ, confirming that both arise in different regions (Robinson, private communication).

O I 1.1287 and 1.3165 μm emission is apparent in the spectrum, with a flux ratio of 1.1287/1.3165$\sim$16.7. This value is far in excess of the ratio of 0.1 expected for UV continuum fluorescence with Lyβ in absorption (Grandi 1975). It therefore appears likely that the O I emission is instead excited by Lyβ

fluorescence, as is the case for MWC349 (KRC94). Following the argument of KRC94 this result implies that Hα is optically thick, and that the O I emission originates in a dense region of material at the H I-H II boundary. KRC94 assume that this zone occurs in a circumstellar disc in MWC349, and suggest the presence of O I emission to be a useful signpost for the presence of a circumstellar disc.

Mg II 2.138/44 μm emission is present, and is thought to be excited via Lyβ fluorescence (Sect. 3). The 2.138/2.144 μm flux ratio $\sim$0.3 suggests that the transitions are optically thin (e.g. MHH88). We tentatively identify C I $\sim$1.0689 μm and N I 1.2469 μm emission in the J band spectrum. Both these species were present in the optical spectra of CI Cam; however a number of N I features of approximately equal strength seen in η Carinae between 1.20–1.23 μm are absent in the spectrum of CI Cam (Hamann et al. 1994).

We find no evidence for H_2 emission, suggesting either that shock heating is relatively unimportant in CI Cam, or that temperatures are sufficiently high to dissociate the molecules. Despite the detection of Mg I emission in the optical spectra, we find no evidence for emission at $\sim$1.578 μm.

5. Discussion

It is clear from the spectra presented here that both stars have rich and complex circumstellar environments, although it is not clear whether this is due to the binarity of both systems, a result of their evolutionary state or a combination of the two. Evidence for the role of binarity is provided by the highly variable He II emission observed in the optical spectra of both objects, possibly the result of X-ray irradiation or heating by an accretion disc. We note that He II emission is not associated with any other known isolated classical Be star or Be/X-ray binary system, although it is apparent in several O supergiant X-ray binaries, such as Cyg X–1 and 4U 1700-37 (Gies & Bolton 1986, Sowers et al. 1998 and Kaper et al. 1994).

Comparison of the I band spectrum of HD 34921 to those of classical Be stars (Andrillat et al. 1988) and the B[e] stars HD 50138 and HD 45677 (Jaschek et al. 1992) shows that it is consistent with an identification as either classical Be or B[e] star. The K band spectrum is found to be qualitatively similar to those of early (B0–B2.5) classical Be stars (Clark & Steele, in prep.); strong He I 2.058 μm and Mg II emission is seen in $\sim$50 per cent and $\sim$40 per cent of classical Be stars respectively. Na I emission is much rarer however, with only 4 stars out of a total sample of 66 showing possible emission features.

Comparison to the K band spectra of the classical Be/X-ray binaries (Fig. 7 and Table 6) shows that none of the classical Be X-ray binaries show evidence for emission from species other than H I and He I (we note that He I emission appears stronger in the classical Be/X-ray binaries than in either HD3492 or the isolated classical Be stars, with emission seen in both He I 2.112 and 2.161 μm, and the EW of He I 2.058 μm exceeding that of Brγ).

The main differences between HD 34921 and the Be X–ray binaries are therefore the presence of variable He II emission,

Table 6. Summary of stellar parameters of the classical Be/ X-ray binaries, line identifications and Equivalent Widths (EW), given in -Å. References for the spectral types are: [a]Lyubimkov et al. (1997), [b] Steele et al. (1998), [c]Negueruela et al. (1996), [d]Coe et al. (1988), [e]Steiner et al. (1984). All spectra were obtained on 1996 October 1–3.

Name	Spectral Type	He I 2.058 μm	He I 2.112 μm	Br γ
X Persei	B0Ve[a]	18.3	2.7	14.5
A0535+26	B0Ve[b]	5.8	-	3.4
4U0728-25	O8-9Ve[c]	6.1	-	1.5
EXO2030+375	B0e[d]	8.4	1.7	4.0
4U2206+54	O9.5IIIpe[e]	-	-1.7(abs)	2.9

and cold gas and dust associated with the circumstellar environment. Cold dust is not associated with any known classical Be/X-ray binary, and from a sample of 101 isolated Be stars only one, 51 Oph, is observed to have an IR excess consistent with dust emission (Waters et al. 1988). Recently Miroshnichenko et al. (1999) have identified 2 additional candidate Be stars which also show evidence for thermal emission from a dusty envelope (HD 4881 and HD 5839); however in all three cases it is likely that these stars are relatively young high mass counterparts of the β Pictoris stars. Although it is not yet certain that the dust is definitely associated with the star, the presence of Na I emission clearly indicates that regions of the circumstellar envelope of HD 34921 are cool and dense enough to prevent ionisation by direct stellar radiation. The low opening angle and large radial density gradient of classical Be stars ($\propto R^{-(2-3)}$; Waters 1986) suggests that the disc density will fall more rapidly than the radiation density, keeping the disc material ionised out to very large radii. Therefore it would appear that either the geometry or radial density gradient of the circumstellar envelope of HD 34921 must differ from that typically seen for a classical Be star (the density of the cool emitting region can be further constrained to $N_H < 10^{10}$ cm^{-3} by noting that neither CO bandhead emission at $\sim$2.3 μm or TiO emission at 6159 Å is seen).

Given the classification criteria of L98 we find that HD 34921 is not luminous enough to be classified as a sgB[e] star, and so we adopt an unclassifiable, unclB[e], "classification" to denote its uncertain evolutionary status. HD 34921 appears to resemble the unclB[e] star HD 45677, which L98 describe as being an example of an extreme Be star since it shares certain spectral properties with classical Be stars while possessing a dusty envelope.

As with HD34921 we find evidence for a highly stratified circumstellar envelope around CI Cam. Given the strength of the H I and He I emission lines there is clearly a dense, ionised wind present; the strong O I emission points to recombination in this wind. Fe II emission suggests that this region has a density $> 10^{5-6}$ cm^{-3} while the [Fe II] line ratio implies the presence of a region(s) with a density of $\leq 10^5$ cm^{-3}. Finally, the presence of Na I and CO bandhead emission indicates that regions of very cold (< 5000 K), dense ($\geq 10^{10}$ cm^{-3}) material are also present. Given the estimated luminosity of CI Cam ($\sim 10^5$ $L_\odot$; Belloni priv. communication) it is instructive to compare it to

other candidate sgB[e] stars and related luminous post Main Sequence objects.

Although few observations of luminous stars in the J and H bands have been made we note that CI Cam strongly resembles the famous LBV η Carinae, with many Fe II, [Fe II] and other metallic emission lines present in addition to emission from H I and He I (Hamann et al. 1994). The unusual object MWC 349, described as unclB[e] by L98 also has a similarly rich near IR spectrum with many metallic emission features. Comparison of CI Cam to the 1 μm spectra of OB stars presented by Conti & Howarth (1999) shows that it most closely resembles the well known LBV P Cygni, with very strong He I 1.08 μm and Paγ emission features.

Strong H I, Mg II, Na I and CO bandhead emission is present in the K band spectrum of CI Cam, and is also seen in the sgB[e] stars S-18 and GG Carinae (although Na I and CO bandhead emission are both present in only one observation of GG Carinae). However, the He I emission is much more pronounced in CI Cam than in these B[e] stars; resembling the LBVs Hen 3–519, R 123 and Wra 751, and the Ofpe star HDE 268840 more closely in this respect. Na I and/or CO bandhead emission is also seen in R 123 and HDE 268840, and also the LBV AG Carinae (Morris et al. 1996, McGregor et al. 1988b). Clearly there is a significant overlap in K band spectral morphology between the different types of luminous post main sequence objects. Indeed AG Carinae has previously been classified as an Ofpe/WN9 star, but the K band spectrum obtained in 1995 shows that by then it closely resembled the sgB[e] stars GG Carinae and S18, as does the LBV R 123 (Morris et al. 1996). Whether this represents a real evolutionary connection between the Ofpe and B[e] stars, and the LBVs is at present unclear. However, despite having spectral similarities with the LBVs, CI Cam is not luminous enough to be classified as an LBV, and equally has not shown the large amplitude long term variability that is characteristic of LBVs. Given its estimated luminosity, rich emission spectrum and the presence of hot dust we prefer the classification of sgB[e] star, and suggest that it may be a close relative of GG Carinae, also a known binary, and possibly the supergiant X-ray binary Wray 977. Kaper et al. (1995) classify the system as B1 Ia+, placing it in the same region of the HR diagram as P Cygni, AG Carinae, and other luminous transitional objects, and recent ISO observations suggest that it also shows an IR excess, possibly arising from cold dust in the circumstellar environment (Kaper et al. 1998). IR spectroscopy of this source to search for signatures of cool ejecta (such as Na I or CO bandhead features) would be usefull to test this possible connection.

Various authors have speculated that binarity may play a role in the B[e] phenomenon and the structure and composition of the circumstellar envelope of B[e] stars. In the light of this speculation we note that recent photometric observations of CI Cam since the 1998 April X–ray to radio flare indicate a long term strengthening of the near IR excess, which arises from the hot circumstellar dust. Possible explanations for this involve a change in the composition of the dust due to reheating by the X-ray flare (van Ancker; private communication) or the forma-tion of new dust in the wake of the outburst (Clark et al., in preparation).

6. Conclusions

The suspected X-ray binaries HD34921/1H0521+37 and CI Cam are proposed as the first candidate HMXB with mass donors showing the B[e] phenomenon. Both stars show clear spectral differences from the classical Be X-ray binaries. With the exception of highly variable He II emission, the optical and UV spectra of 1H0521+37 closely resemble those of the classical Be X-ray binaries X Persei and A0535+26. The I band spectrum, showing double peaked Paschen emission is again characteristic of classical Be stars. However, the K band spectra show evidence for the presence of cold ejecta within the system, with narrow Na I emission features observed. Likewise archival IRAS observations of the field suggest emission from an envelope of cold dust, neither of which are characteristic of either isolated or binary classical Be stars.

CI Cam has a very rich near IR emission line spectrum, closely resembling those of the LBVs, sgB[e] stars and other luminous post Main Sequence objects. Many distinct regions of the circumstellar environment are identifiable, with a highly excited region in the vicinity of the compact object object indicated by He II emission, presumably embedded in the dense stellar wind of the mass donor. Na I and CO bandhead emission are both indicative of dense, cold regions of the circumstellar envelope; whether these are located in a circumstellar disc as is suggested for the sgB[e] stars, or are a result of discrete mass ejections, possibly triggered by the presence of the compact object is as yet unclear.

References

Andrillat Y., Jaschek M., Jaschek C., 1988, A&AS 72, 129

Coe M.J., Payne B.J., Longmore A., Hanson C.G., 1988, MNRAS 232, 865

Conti P.S., Howarth I.D., 1999, MNRAS 302, 145

Downes R.A., 1984, PASP 96, 807

Everall C., 1995, Ph.D. Thesis, University of Southampton

Gies D.R., Bolton C.T., 1986, ApJ 304, 389

Grandi S.A., 1975, ApJ 196, 465

Hamann F., Simon M., 1986, ApJ 311, 909

Hamann F., DePoy D.L., Johansson S., Elias J., 1994, ApJ 422, 626

Hanson M.M., Conti P.S., Rieke M.J., 1996, ApJS 107, 281 (H96)

Hjellming R.M., Mioduszewski A.J., 1998, IAUC 6857

Jaschek M., Jaschek C., Andrillat Y., Houziaux L., 1992, MNRAS 254, 413

Kaper L., Hammerschlag–Hensberge G., Zuiderwijk E.J., 1994, A&A 289, 846

Kaper L., Lamers H.J.G.L.M., Ruymaekers E., van den Heuvel E.P.J., Zuiderwijk E.J., 1995, A&A 300, 446

Kaper L., Trams N.R., Barr P., van Loon J.Th., Waters L.B.F.M., 1998, Ap&SS 255, 199

Kelly D.M., Rieke G.H., Campbell B., 1994, ApJ 425, 231 (KRC94)

Lamers H.J.G.L.M., Zickgraf F.–J., de Winter D., Houziaux L., Zorec J., 1998, A&A 340, 117 (L98)

Lyubmikov L.S., Rostopchin S.I., Roche P., Tarasov A.E., 1997, MN-RAS 286, 895

Maeder A., Maynet A., 1989, A&A 210, 155

McGregor P.J., Hyland A.R., Hillier D., 1988, ApJ 324, 1071 (MHH88)

McGregor P.J., Hillier D., Hyland A.R., 1988b, ApJ 334, 639

Miroshnichenko A.S., Mulliss C.L., Bjorkman K.S., et al., 1999, MN-RAS 302, 612

Mountain C.M., Robertson D.J., Lee T.J., Wade R., 1990, SPIE 1235, 25

Morris P.W., Eenens P.R.J., Hanson M.M., Conti P.S., Blum R.D., 1996, ApJ 470, 597

Negueruela I., Roche P., Buckley D.A.H., et al., 1996, A&A 315, 160

Oudmaijer R.D., Waters L.B.F.M., van der Veen W.E.C.J., Geballe T.R., 1995, A&A 299, 69

Polcaro V.F., et al., 1990, A&A 231, 354

Puxley P.J., Beard S.M., Ramsay S.K., 1992, In: Data Analysis Workshop-4th ESO/ST-ECF Garching, p. 117

Scoville N.Z., Krotkov R., Wang D., 1980, ApJ 240, 929

Smith D., Reillard R., Swank J., Takeshima T., Smith E., 1998, IAUC 6855

Soifer B.T., Rice W.L., Mould J.R., et al., 1986, ApJ 304, 651

Sowers J.W., Gies D.R., Bagnuolo W.G., et al., 1998, ApJ 506, 424

Steele I.A., Negueruela I., Coe M.J., Roche P., 1998, MNRAS 297, L5

Steiner J.E., Ferrara A., Garcia M., et al., 1984, ApJ 280, 688

Wagner R.M., Starrfield S.G., 1998, IAUC 6857

Waters L.B.F.M., 1986, A&A 162, 121

Waters L.B.F.M., Cote J., Geballe T.R., 1988, A&A 203, 348

Zickgraff F.-J., Wolf B., Stahl O., Leitherer C., Klare G., 1985, A&A 143, 421